

头颈部肿瘤 CT 灌注成像与微血管密度(MVD)的相关性研究

王杰¹ 唐作华^{1△} 王纾宜² 曾文娇³ 钱雯¹ 吴灵捷¹ 王文忠¹ 罗剑锋⁴

(¹ 复旦大学附属眼耳鼻喉科医院放射科, ² 病理科 上海 200031; ³ 复旦大学基础医学院病理学系 上海 200032;

⁴ 复旦大学公共卫生学院卫生统计与社会医学教研室 上海 200032)

【摘要】目的 研究头颈部肿瘤 CT 灌注成像和微血管密度(microvessel density, MVD)的相关性,探讨其在评价肿瘤血管丰富程度及鉴别良、恶性肿瘤中的应用价值。**方法** 将 41 例头颈部肿瘤分成 3 组:A 组 16 例,良性乏血供肿瘤;B 组 13 例,良性富血供肿瘤;C 组 12 例,恶性肿瘤。术前对所有肿瘤行 CT 灌注检查,用后处理软件绘制时间-密度曲线(time density curve, TDC),并计算感兴趣区的最大密度投影(maximum intensity projection, MIP)、血容量(blood volume, BV)、血流量(blood flow, BF)、平均通过时间(mean transit time, MTT)和毛细血管通透性(capillary permeability, CP)等参数。同时切取与 CT 灌注相同层面的组织切片,行 CD34 抗体免疫组织化学染色,观察分析各 CT 灌注成像在 3 组肿瘤之间表现的差异及其与 MVD 的相关性。**结果** 头颈部肿瘤 CT 灌注成像 TDC 显示,良性肿瘤(A 组+B 组)出现 I 型 TDC 的频率明显高于恶性肿瘤(C 组)($P=0.003$),恶性肿瘤中以 II 型和 III 型 TDC 为主。B 组和 C 组的 MIP、BV 及 BF 均比 A 组明显高($P<0.01$)。MVD 在 3 组肿瘤之间差异无统计学意义($P>0.05$)。Pearson 相关性分析表明在 3 组肿瘤中 MVD 与 MIP、BV 均呈正相关($P<0.05$, r 值分别为 0.41, 0.352)。**结论** CT 灌注成像的 TDC 形态、MIP 和 BV 等可间接反映头颈部肿瘤血管生成情况,结合 MVD 有助于鉴别良性乏血供肿瘤、良性富血供肿瘤及恶性肿瘤。

【关键词】 头颈部肿瘤; 体层摄影术,X 线计算机; 灌注成像; 微血管密度(MVD)

【中图分类号】 R 445 **【文献标志码】** A **doi:** 10.3969/j.issn.1672-8467.2014.05.003

Head and neck neoplasms:correlation of CT perfusion with microvessel density (MVD)

WANG Jie¹, TANG Zuo-hua^{1△}, WANG Shu-yi², ZENG Wen-jiao³,
QIAN Wen¹, WU Ling-jie¹, WANG Wen-zhong¹, LUO Jian-feng⁴

(¹ Department of Radiology, ² Department of Pathology, Eye, Ears, Nose and Throat Hospital, Fudan University, Shanghai 200031, China; ³ Department of Pathology, School of Basic Medical Sciences, Fudan University, Shanghai 200032, China;

⁴ Department of Health Statistics and Social Medicine, School of Public Health, Fudan University, Shanghai 200032, China)

【Abstract】 Objective To evaluate the correlation between CT perfusion (CTP) and microvessel density (MVD) in head and neck neoplasms (HNNs), and to assess its value in the differential diagnosis of benign HNNs from malignant ones. **Methods** Forty-one HNNs proved by pathology underwent CTP before the operation. All lesions were divided into three groups: group A (sixteen cases), benign hypovascular lesions; group B (thirteen cases), benign hypervascular lesions; group C

(twelve cases), malignant lesions. Time density curve (TDC) and CTP parameters including maximum intensity projection (MIP), blood volume (BV), blood flow (BF), mean transit time (MTT), and capillary permeability (CP) were analyzed respectively. Tissue slices from the same level as CT perfusion were used for anti-CD34 immunohistochemical staining and MVD counts. The relation between perfusion measurements and MVD were analyzed. **Results** TDC could be classified into three types. TDC of type I was more frequently found in benign lesions (group A and B) than in malignant lesions (group C) ($P = 0.003$), while type II and type III were mainly found in group C. MIP, BV and BF were all significantly higher in both group B and C than group A (all $P < 0.01$). There was no statistically significant difference in MVD among the three groups ($P > 0.05$). Pearson correlation showed a positive correlation between MVD and MIP, BV respectively among the three groups (all $P < 0.05$, $r = 0.41, 0.352$). **Conclusions** TDC, MIP and BV of CTP could reflect angiogenesis of HNNs indirectly. CTP combined with MVD could help differentiating malignant from benign HNNs, as well as benign hypovascular from hypervascular ones.

【Key words】 head and neck neoplasms; tomography, X-ray computed; perfusion imaging; microvessel density

* This work was supported by the Crossover Study Fund of Basic & Clinical Medicine of Shanghai Medical College of Fudan University (Z-259).

肿瘤血管生成在肿瘤的发生、发展及转移过程中起关键作用^[1-2]。多项研究表明在头颈部肿瘤患者中,肿瘤血管生成会增加局部复发和远处转移的风险,降低生存率,显著影响患者的预后^[3-5]。CT灌注成像作为一种功能成像技术可以活体评估肿瘤组织的血流供应情况,从而间接反映肿瘤血管生成的丰富程度^[6-8]。肿瘤内微血管密度(microvessel density, MVD)代表了肿瘤新生血管的丰富程度^[9-10],研究报道MVD和头颈部肿瘤患者的预后密切相关,较高的MVD可提示预后不良,然而MVD测定需依赖活体组织^[1,9,11]。本文收集41例头颈部肿瘤患者资料,探讨CT灌注成像表现与MVD的相关性,旨在从全新的角度探讨头颈部肿瘤的影像学表现和分子生物学特性之间的关系,从而为临床诊断、治疗和估计预后提供更多的信息。

材料和方法

病例资料 此前瞻性研究已获得复旦大学附属眼耳鼻喉科医院伦理审查委员会的批准,且在试验前获得患者的书面知情同意书。本研究包括头颈部肿瘤患者41例,其中男23例,女18例,年龄22~74岁。原发肿瘤包括腮腺20例、颞骨11例(外耳道7例,乳突部3例及岩尖部1例)、咽旁间隙7例、颞下窝1例、颈静脉孔1例和翼腭窝1例。所有肿

瘤的手术标本均经组织病理学诊断,且被分成了3组(A组16例,良性乏血供肿瘤;B组13例,良性富血供肿瘤;C组12例,恶性肿瘤)。

CT扫描 试验采用16排西门子螺旋CT机进行扫描成像。所有病例于CT灌注扫描前行CT平扫,选取肿瘤最大直径相邻两层作为靶层面行CT灌注扫描(避开大片钙化和囊变区)。使用高压注射器经肘静脉注入50 mL对比剂(碘帕醇,300 mg/mL),注射速率4 mL/s。注药4 s后开始动态CT扫描,扫描参数:120 kV/100 mA,层厚12 mm×2,时间间隔1 s,总共扫描时间40 s。灌注扫描结束后3 min行常规增强扫描,参数如下:120 kV/180 mA,层厚5 mm,矩阵512×512,视野230 mm×230 mm。

将灌注扫描所得图像传到西门子工作站,根据Patlak算法用Perfusion软件中的体部肿瘤程序进行计算。所有图像分析过程由2名双盲的头颈部影像医师共同完成。将同侧颈内或颈外动脉作为输入动脉,生成最大密度投影(maximum intensity projection, MIP)、血容量(blood volume, BV)、血流量(blood flow, BF)、平均通过时间(mean transit time, MTT)和毛细血管通透性(capillary permeability, CP)等灌注参数的伪彩图。选取肿瘤直径最大的层面,若肿瘤均匀强化,则感兴趣区(region of interest, ROI)至少包括所选层面肿瘤50%的面积;若肿瘤不均匀强化,则以肿瘤强化最明

显处为 ROI, 避开明显的血管、坏死囊变区和钙化灶, 选 3 次取平均值^[12]。最后获得所选 ROI 的时间—密度曲线 (time density curve, TDC) 和 MIP、BV、BF、MTT、CP 等 CT 灌注参数值。

免疫组化检查 所有患者在 CT 灌注检查后均尽快行肿瘤切除术, 手术标本用 4% 甲醛固定, 将标本按 CT 扫描的位置摆放, 在肿瘤最大直径层面切取厚 3~5 mm 的标本并制成蜡块备用。将石蜡包埋标本制成 4 μm 厚的切片, 每例连续 2 张切片, 1 张用于常规苏木精-伊红 (HE) 染色, 另 1 张用于鼠抗人 CD34 单克隆抗体 (福州迈新生物技术有限公司) 染色并进行 MVD 计数。先在低倍镜下 ($\times 40$) 选取 5 个肿瘤血管最丰富的视野, 其中 3 个在肿瘤的中心部位, 2 个位于肿瘤的边缘部位, 同时避免坏死等区域。在高倍镜 ($\times 200$) 下分别观察所选的 5 个视野, 用 I-Solution 软件 (加拿大 NatureGene 公司) 自动计算每个视野中血管所占面积的百分比并计算 5 个视野的平均值^[12]。

统计学分析 采用 SPSS16.0 统计软件对所得数据进行分析。不同类型 TDC 在 3 组肿瘤间的分布差异用 Fisher 确切概率法检验, 3 组肿瘤之间灌

注参数的比较用非参数 Mann-Whitney 检验, 用 Pearson 相关系数来评估 MVD 与各灌注参数的相关性。 $P < 0.05$ 为差异有统计学意义。

结 果

头颈部肿瘤的 TDC 形态 根据达峰时间 (time to peak, TTP) 和廓清指数 (washout ratio, WR), 将 TDC 分成 3 种类型^[13]。其中, TTP 为达到强化峰值所需的时间; $WR(\%) = (强化峰值 - 注入造影剂 44 s 后的密度) / (强化峰值 - 注入造影剂前的密度) \times 100\%$ 。I 型 TDC (缓慢上升型, 图 1) 的 $TTP > 30$ s 且 $WR \leq 0$; II 型 TDC (速升速降型, 图 2) 的 $TTP \leq 30$ s 且 $WR > 30\%$; III 型 TDC (速升缓降型) 的 $TTP \leq 30$ s 且 $WR \leq 30\%$ 。3 组肿瘤 TDC 走势类型见表 1。A 组出现 I 型 TDC 的频率明显高于 B 组和 C 组 ($P = 0.003, 0.000$)。II 型 TDC 仅在 B 组和 C 组中出现。III 型 TDC 的出现频率在 3 组间差异无统计学意义。良性肿瘤 (A 组 + B 组) 出现 I 型 TDC 的频率明显高于恶性肿瘤 (C 组), 良、恶性肿瘤出现 I 型 TDC 频率的差异有统计学意义 ($P = 0.003$), 恶性肿瘤以 II 型和 III 型曲线为主。

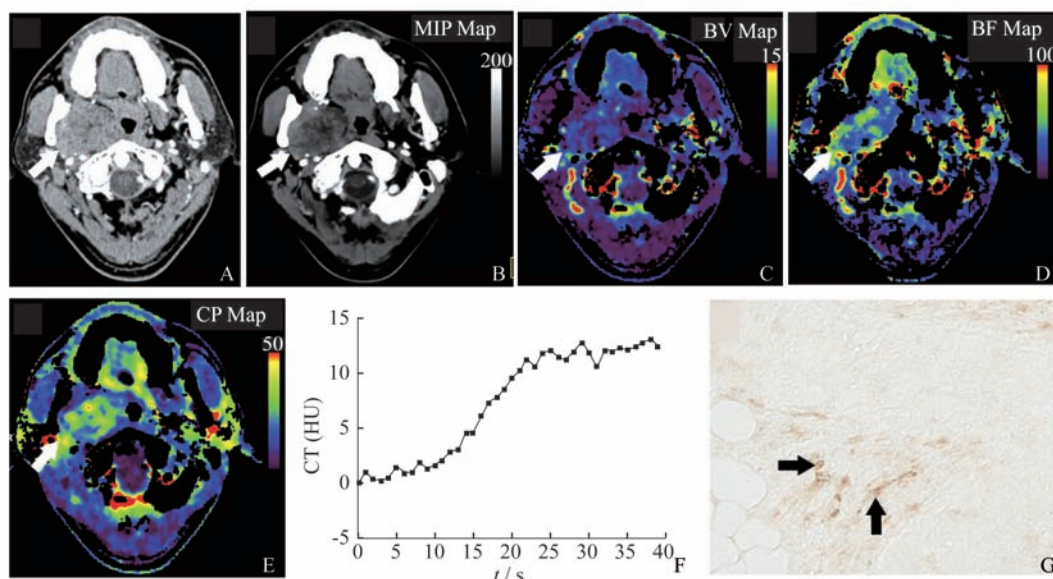


图 1 A 组多形性腺瘤的 CT 灌注伪彩图及微血管染色结果

Fig 1 CTP functional maps and microvessel staining of pleomorphic adenoma of group A

A fifty-year-old male patient with pleomorphic adenoma of the right parapharyngeal space (white arrows). Axial contrast-enhanced CT (A), MIP (B), BV (C), BF (D), CP (E), TDC (F) as well as CD34 immunohistochemical staining (G) of the tumor are shown. The well-defined mass has heterogeneous enhancement (A), and the areas with obvious enhancement have higher MIP (B), BV (C), BF (D), and CP (E) values compared with the ipsilateral masseter. TDC of type I has a relatively slow ascending phase without descending phase (F). Note the poor degree of angiogenesis in the tumor parenchyma. The vascular endothelial cells are stained as brown arrows ($\times 200$) (G).

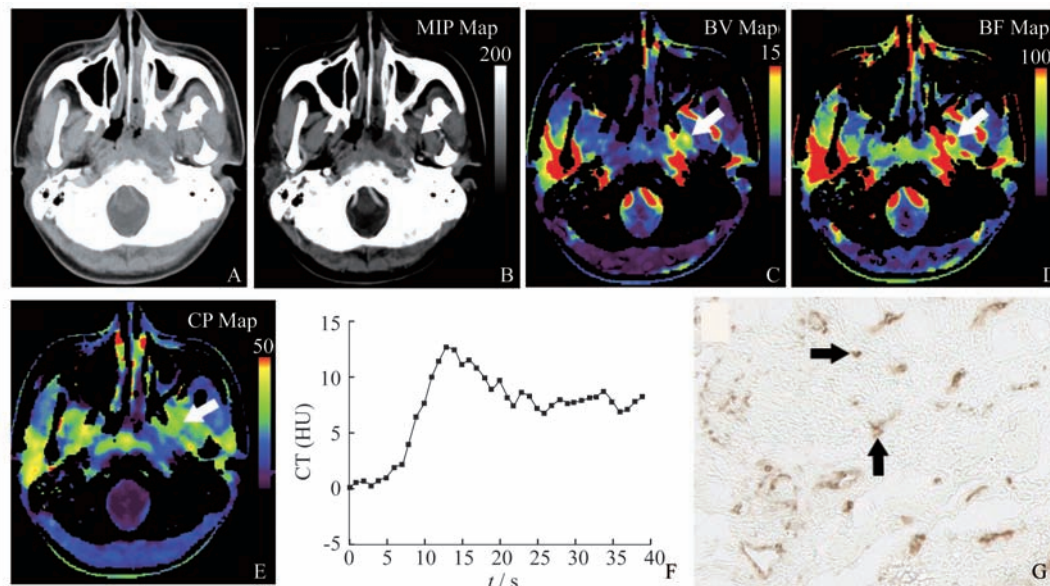


图 2 C 组横纹肌肉瘤 CT 灌注伪彩图及微血管染色结果

Fig 2 CTP functional maps and microvessel staining of rhabdomyosarcoma of group C

A twenty two-year-old male patient with rhabdomyosarcoma of the left parapharyngeal space (white arrows). Axial contrast-enhanced CT (A), MIP (B), BV (C), BF (D), CP (E), TDC (F) as well as CD34 immunohistochemical staining (G) of the tumor are shown. The lesion has higher MIP (B), BV (C), BF (D), and CP (E) values compared with the ipsilateral masseter. TDC of type II has steep ascending and descending phases (F). Note the abundant degree of angiogenesis in the tumor parenchyma. The vascular endothelial cells are stained as brown arrows ($\times 200$) (G).

表 1 41 例病例的病理诊断及 TDC 类型

Tab 1 Histopathologic diagnosis and types of TDC in 41 patients

Histopathologic diagnosis	No. of case	Type I	Type II	Type III
Benign lesions (groups A + B)	29	14	4	11
Benign hypovascular lesions (group A)	16	12	0	4
Pleomorphic adenoma	9	6	0	3
Lymphoepithelial cyst	2	2	0	0
Bronchial cleft cyst	2	2	0	0
Schwannoma	1	1	0	0
Venous hemangioma	1	1	0	0
Osteochondroma	1	0	0	1
Benign hypervascular lesions (group B)	13	2	4	7
Kimura's disease	3	0	0	3
Warthin's tumor	2	0	2	0
Papillary epithelioma	2	0	2	0
Intradermal nevus	1	0	0	1
Chondroblastoma	1	0	0	1
Glomus tumor	1	1	0	0
Granulosa cell tumor	1	0	0	1
Basal cell adenoma	1	0	0	1
Giant cell granuloma	1	1	0	0

(续表 1)

Malignant lesions (group C)	12	0	6	6
Rhabdomyosarcoma	2	0	2	0
Adenoid cystic carcinoma	2	0	0	2
Malignant schwannoma	2	0	1	1
Mucoepidermoid carcinoma	1	0	1	0
Squamous cell carcinoma	2	0	2	0
WDC	1	0	0	1
Epithelioid sarcoma	1	0	0	1
MEMT	1	0	0	1

WDC: Well differentiated chondrosarcoma; MEMT: Metastatic epithelial malignant tumor.

3 组肿瘤之间 CT 灌注参数及 MVD 的比较

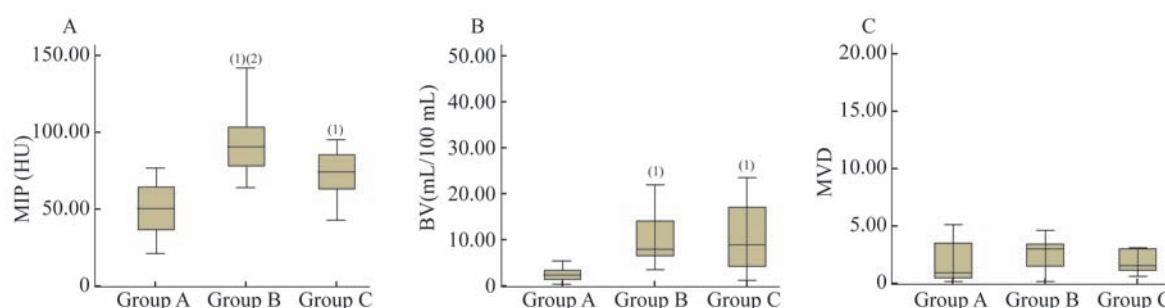
各灌注参数及 MVD 在 3 组之间的比较结果见表 2 和图 3。B 组和 C 组的 MIP、BV 及 BF 均比 A 组明显高($P < 0.01$)；B 组的 CP 值比 A 组明显高($P =$

0.002)；B 组的 MIP 值比 C 组高($P = 0.044$)，但两组间的数据有重叠。MTT 值和 MVD 在 3 组间的差异无统计学意义。良、恶性肿瘤之间的 CT 灌注参数差异无明显统计学意义。

表 2 CT 灌注参数和 MVD 在 3 组间的比较**Tab 2 Comparison of perfusion parameters and MVD in the three groups**

Group	Mann-whitney test	MIP	BV	BF	MTT	CP	MVD
A vs. B	Z	-3.667	-3.946	-3.992	-1.323	-3.064	-1.439
	P	0.000	0.000	0.000	0.186	0.002	0.150
A vs. C	Z	-2.693	-3.389	-3.296	-0.882	-1.811	-1.161
	P	0.007	0.001	0.001	0.378	0.070	0.246
B vs. C	Z	-2.013	-0.272	-0.761	-0.082	-0.870	-1.088
	P	0.044	0.786	0.446	0.935	0.384	0.277
(A+B) vs. C	Z	-0.602	-1.948	-1.633	-0.501	-0.659	-0.143
	P	0.547	0.051	0.102	0.616	0.510	0.886

A: Benign hypovascular lesions; B: Benign hypervascular lesions; C: Malignant lesions. MIP: HU; BV: mL · 100 mL⁻¹; BF: mL · 100 mL⁻¹ · min⁻¹; MTT: s; CP: mL · 100 mL⁻¹ · min⁻¹.

**图 3 3 组肿瘤之间 MIP (A), BV (B) 和 MVD (C) 的比较****Fig 3 The comparison of MIP (A), BV (B) and MVD (C) among the three groups**vs. group A,⁽¹⁾ $P < 0.01$; vs. group C,⁽²⁾ $P < 0.05$.

MVD 与各灌注参数的关系 MVD 与各灌注参数的关系见表 3。在 A 组中 MVD 仅与 MIP 呈正相关($r = 0.526, P = 0.036$)；B 组中 MVD 和 CT 灌注参数均无相关性；C 组中 MVD 与 MIP、BV、BF

均呈正相关(r 分别为 $0.831, 0.855, 0.591, P$ 值分别为 $0.001, 0.000, 0.043$)。在 3 组中, MVD 与 MIP、BV 均有较明显正相关性(r 分别为 $0.41, 0.352, P$ 值分别为 $0.008, 0.024$)。

表3 CT灌注参数与MVD的相关性

Tab 3 Correlation between CT perfusion parameters and MVD

Group	Pearson corelation	MIP	BV	BF	MTT	CP
A	<i>r</i>	0.526	-0.008	-0.186	0.365	-0.228
	<i>P</i>	0.036	0.976	0.490	0.165	0.395
B	<i>r</i>	-0.231	-0.409	-0.413	-0.258	0.059
	<i>P</i>	0.448	0.165	0.160	0.395	0.849
C	<i>r</i>	0.831	0.855	0.591	0.156	-0.092
	<i>P</i>	0.001	0.000	0.043	0.627	0.776
A+B+C	<i>r</i>	0.410	0.352	0.228	0.067	0.005
	<i>P</i>	0.008	0.024	0.150	0.700	0.980

A: Benign hypovascular lesions; B: Benign hypervascular lesions; C: Malignant lesions. MIP: HU; BV: mL·100 mL⁻¹; BF: mL·100 mL⁻¹·min⁻¹; MTT: s; CP: mL·100 mL⁻¹·min⁻¹. In group A, MVD is positively correlated with MIP; In group C, MVD is positively correlated with MIP, BV and BF; In all groups, MVD is positively correlated with MIP and BV.

讨 论

头颈部肿瘤灌注TDC的形态 CT灌注成像可以评估头颈部肿瘤的血供情况,不同的TDC形态主要反映了肿瘤血流灌注的差异^[14],从而进一步反映肿瘤微循环情况。本组实验结果显示,良性乏血供肿瘤(A组)出现I型TDC的频率明显高于良性富血供肿瘤(B组),即I型TDC可以帮助鉴别良性乏血供和富血供肿瘤。此外,良性肿瘤(A+B组)出现I型TDC(缓慢上升型)频率明显高于恶性肿瘤(C组)(*P*=0.003),可能是由于良性肿瘤尤其是良性乏血供肿瘤血液供应相对较少,血管壁较完整^[14],故I型TDC还有助于鉴别头颈部良、恶性肿瘤。恶性肿瘤以II型(速升速降型)和III型(速升缓降型)曲线为主,且II型TDC仅在B组和C组中出现。恶性肿瘤内新生血管丰富,血管内皮细胞连接松散,内皮基底膜发育不完善^[14],对比剂快速进入后又快速流出,形成一尖波峰,故II型TDC可以帮助鉴别良性乏血供肿瘤与良性富血供肿瘤及恶性肿瘤。B组内的某些肿瘤如Warthin瘤和乳头状瘤的TDC形态也为II型,可能与其内毛细血管网较丰富且血管壁不完整有关^[15]。因此,TDC的不同形态可以反映血管微循环的改变,进而帮助鉴别头颈部良、恶性肿瘤。

头颈部肿瘤的CT灌注参数 关于CT灌注参数鉴别头颈部良、恶性肿瘤有不同的研究报道^[14,16-17]。Rumboldt等^[16]的研究表明头颈部良性肿瘤较恶性肿瘤有较低的BF值及较高的MTT

值。然而,Bisdas等^[17]报道腮腺良性肿瘤的BV和BF值比恶性肿瘤明显高。与此两种观点不同,杨智云等^[14]认为头颈部良、恶性肿瘤之间的CT灌注参数差异无统计学意义。我们的结果与其结果一致。另外,良性富血供肿瘤(B组)和恶性肿瘤(C组)的MIP,BV及BF值均明显高于良性乏血供肿瘤(A组)明显高(*P*均<0.01)。MIP参数能反映灌注状态的整体水平和平均程度^[18],由于B组和C组较A组新生血管更丰富,其整体灌注程度更明显,故MIP值增高。B组和C组的BV值明显增高反映了肿瘤内丰富的新生血管所导致的血管床增加;BF值增高则反映了B组和C组内新生血管有大量动静脉分流^[19]。因此,MIP、BV和BF可以反映头颈部肿瘤血管生成的丰富程度,据此可以将良性乏血供肿瘤分别与良性富血供肿瘤及恶性肿瘤进行鉴别。然而,BV和BF在B组和C组之间差异无统计学意义(*P*>0.05)。原因可能是良性富血供肿瘤内有很多微血管,且其细胞及基质的含量也较丰富,从而导致较高的MIP、BV和BF值;同时,恶性肿瘤中的坏死部分会明显影响CT灌注成像参数^[17],引起MIP、BV和BF值降低。另外,B组的CP值比A组明显高(*P*=0.002),可能与B组中某些肿瘤如Warthin瘤和乳头状瘤血管壁不完整,导致肿瘤血管的通透性增加有关^[15],从而有助于鉴别良性乏血供与富血供肿瘤。

头颈部肿瘤的MVD及其与CT灌注成像表现的关系 目前广泛认为肿瘤血管生成对肿瘤生长有极其重要的作用^[20],而MVD是反映肿瘤新生血管的“金标准”^[9-10],有研究认为MVD可间接反映肿

瘤的恶性程度^[21]。然而,本组实验中MVD在3组肿瘤间差异无统计学意义,与杨智云等^[14]和Li等^[22]等的研究结果一致。原因可能为不同病理类型的肿瘤血供差异大、血管丰富程度相近所致^[14],另外MVD计数和组织取材的误差也会影响实验结果。因此,我们不能仅依据肿瘤局部MVD来帮助鉴别头颈部肿瘤的良、恶性情况。

CT灌注参数可以定量评估肿瘤的血管生成情况,且其可有效评估抗血管生成药物的化疗疗效^[23~24]。因此,CT灌注参数与肿瘤血管生成的组织学指标MVD之间可能有一些相关性。Ash等^[1]证实了头颈部鳞癌中MVD分别和BV及BF呈正相关,杨智云等^[14]也证明了头颈部肿瘤中MVD与BF等参数呈正相关。本研究显示在A组中MVD与MIP呈正相关,C组中MVD与MIP、BV、BF均呈正相关,虽然在B组中MVD与CT灌注参数无相关性,但在所有3组中MVD与MIP、BV均有较明显的正相关性,可能由于不同组肿瘤的血管生成情况及微循环不同所造成。因此,MVD结合CT灌注参数可将良性乏血供肿瘤分别与良性富血供肿瘤及恶性肿瘤进行区分,并且由于I型TDC可鉴别良、恶性肿瘤,故MVD结合CT灌注成像表现可进一步鉴别这3组肿瘤。

本研究尚有一些缺点与不足之处。首先,由于样本量较小及3组肿瘤的CT灌注参数数据有部分重叠,故需要增加样本量来进一步证实CT灌注成像在评估头颈部肿瘤血管生成情况中的作用;其次,本实验中CT灌注扫描时间仅为40 s,较长的扫描时间可以提供更多的反映肿瘤微循环的信息;再次,我们的研究使用的是16排螺旋CT,使用更高排数的CT机可以获得更精确的数据。

总之,本组研究表明CT灌注成像可以鉴别良性乏血供肿瘤、良性富血供肿瘤及恶性肿瘤,且在所有3组中MIP、BV均和MVD呈正相关,即CT灌注可评估头颈部肿瘤血管生成情况,从而为临床治疗方法选择、疗效判定及预后评估提供更加客观的依据。

参 考 文 献

- [1] Ash L, Teknos TN, Gandhi D, et al. Head and neck squamous cell carcinoma: CT perfusion can help noninvasively predict intratumoural microvessel density [J]. *Radiology*, 2009, 251(2):422~428.
- [2] Lee TY, Purdie TG, Stewart E. CT imaging of angiogenesis[J]. *Q J Nucl Med*, 2003, 47(3):171~187.
- [3] Li C, Fan J, Song X, et al. Expression of angiopoietin-2 and vascular endothelial growth factor receptor-3 correlates with lymphangiogenesis and angiogenesis and affects survival of oral squamous cell carcinoma[J]. *PLoS One*, 2013, 8(9):e75388.
- [4] Dai W, Li Y, Zhou Q, et al. Cetuximab inhibits oral squamous cell carcinoma invasion and metastasis via degradation of epidermal growth factor receptor [J]. *J Oral Pathol Med*, 2014, 43(4):250~257.
- [5] de Oliveira MV, Pereira Gomes EP, Pereira CS, et al. Prognostic value of microvessel density and p53 expression on the locoregional metastasis and survival of the patients with head and neck squamous cell carcinoma [J]. *Appl Immunohistochem Mol Morphol*, 2013, 21(5):444~451.
- [6] Meijerink MR, van Waesberghe JHTM, van der Weide L, et al. Total-liver-volume perfusion CT using 3-D image fusion to improve detection and characterization of liver metastases[J]. *Eur Radiol*, 2008, 18(10):2345~2354.
- [7] Yi CA, Lee KS, Kim EA, et al. Solitary pulmonary nodules: dynamic enhanced multi-detector row CT study and comparison with vascular endothelial growth factor and microvessel density[J]. *Radiology*, 2004, 233(1):191~199.
- [8] Trojanowska A, Trojanowski P, Drop A, et al. Head and neck cancer: value of perfusion CT in depicting primary tumor spread[J]. *Med Sci Monit*, 2012, 18(2):CR112~CR118.
- [9] Choi JY, Jang KT, Shim YM, et al. Prognostic significance of vascular endothelial growth factor expression and microvessel density in esophageal squamous cell carcinoma: comparison with positron emission tomography[J]. *Ann Surg Oncol*, 2006, 13(8):1054~1062.
- [10] Yamahatsu K, Matsuda Y, Ishiwata T, et al. Nestin as a novel therapeutic target for pancreatic cancer via tumor angiogenesis[J]. *Int J Oncol*, 2012, 40(5):1345~1357.
- [11] Chen TW, Yang ZG, Chen HJ, et al. Quantitative assessment of first-pass perfusion using a low-dose method at multidetector CT in oesophageal squamous cell carcinoma: correlation with VEGF expression[J]. *Clin Radiol*, 2012, 67(8):746~753.
- [12] d'Assignies G, Couvelard A, Bahrami S, et al. Pancreatic endocrine tumours: tumour blood flow assessed with perfusion CT reflects angiogenesis and correlates with prognostic factors [J]. *Radiology*, 2009, 250(2):407~416.
- [13] Dong Y, Lei GW, Wang SW, et al. Diagnostic value of CT perfusion imaging for parotid neoplasms[J]. *Dentomaxillofac Radiol*, 2014, 43(1):20130237.
- [14] 杨智云,孟俊非,徐巧兰,等.头颈部肿瘤CT灌注成像表现与微血管生成因子表达水平的相关性研究[J].中华放射学杂志,2007,41(9):900~906.
- [15] Woo SH, Choi DS, Kim JP, et al. Two-phase computed

- tomography study of warthin tumour of parotid gland: differentiation from other parotid gland tumours and its pathologic explanation [J]. *J Comput Assist Tomogr*, 2013, 37(4):518–524.
- [16] Rumboldt Z, Al-Okaili R, Deveikis JP. Perfusion CT for head and neck tumours: pilot study [J]. *AJNR Am J Neuroradiol*, 2005, 26(5):1178–1185.
- [17] Bisdas S, Baghi M, Wagenblast J, et al. Differentiation of benign and malignant parotid tumours using deconvolution-based perfusion CT imaging: feasibility of the method and initial results [J]. *Eur J Radiol*, 2007, 64(2):258–265.
- [18] 李春志, 韩丹, 宋光义, 等. 双源CT灌注成像诊断胃癌的初步研究[J]. 中国医学影像技术杂志, 2009, 17(5):329–332.
- [19] Feng ST, Sun CH, Li ZP, et al. Evaluation of angiogenesis in colorectal carcinoma with multidetector-row CT multislice perfusion imaging [J]. *Eur J Radiol*, 2010, 75(2):191–196.
- [20] George ML, Dzik-Jurasz AS, Padhani AR, et al. Non-invasive methods of assessing angiogenesis and their value in predicting response to treatment in colorectal cancer [J]. *Br J Surg*, 2001, 88(12):1628–1636.
- [21] Cuenod CA, Fournier L, Balvay D, et al. Tumour angiogenesis: pathophysiology and implications for contrast-enhanced MRI and CT assessment [J]. *Abdom Imaging*, 2006, 31(2):188–193.
- [22] Li ZP, Meng QF, Sun CH, et al. Tumour angiogenesis and dynamic CT in colorectal carcinoma: radiologic-pathologic correlation [J]. *World J Gastroenterol*, 2005, 11(9):1287–1291.
- [23] Sahani DV, Kalva SP, Hamberg LM, et al. Assessing tumour perfusion and treatment response in rectal cancer with multisection CT: initial observations [J]. *Radiology*, 2005, 234(3):785–792.
- [24] Ng QS, Goh V, Milner J, et al. Effect of nitric oxide synthesis on tumour blood volume and vascular activity: a phase I study [J]. *Lancet Oncol*, 2007, 8(2):111–118.

(收稿日期:2014-02-22;编辑:王蔚)

(上接第 580 页)

- [7] 范存义, 汤林翔. 负载妥布霉素的硫酸钙治疗慢性骨髓炎及合并骨缺损的疗效评价. [J]. 中华创伤骨科杂志, 2005, 7(10):954–955.
- [8] 徐华梓, 应小樟, 吴银生, 等. 利福平硫酸钙植入剂的活体内药代动力学研究[J]. 脊柱外科杂志, 2007, 5(5):290–297.
- [9] Gervasini G, Garcia M, Macias RM, et al. Impact of genetic polymorphisms on tacrolimus pharmacokinetics and the clinical outcome of renal transplantation [J]. *Transpl Int*, 2012, 25(4):471–480.
- [10] Asano T, Takahashi KA, Fujioka M, et al. ABCB1C3435T and G2677T/A polymorphism decreased the risk for steroid-induced osteonecrosis of the femoral head after kidney transplantation [J]. *Pharmacogenetics*, 2003, 13(11):675–682.
- [11] Chen CH, Uang YS, Wang ST, et al. Interaction between Red Yeast Rice and CYP450 Enzymes/P-Glycoprotein and its Implication for the Clinical Pharmacokinetics of Lovastatin [J]. *Evid Based Complement Alternat Med*, 2012, 127043.
- [12] Azzariti A, Porcelli L, Quatrone AE, et al. The coordinated role of CYP450 enzymes and P-gp in determining cancer resistance to chemotherapy [J]. *Curr Drug Metab*, 2011, 12(8):713–721.
- [13] Mitin T, VonMoltke LL, Court MH, et al. Levothyroxine upregulates P-glycoprotein independent of the pregnane X receptor [J]. *Drug Metab Dispos*, 2004, 32(8):779–782.
- [14] Maier A, Zimmermann C, Beglinger C, et al. Effects of budesonide on P-glycoprotein expression in intestinal cell lines [J]. *Br J Pharmacol*, 2007, 150(3):361–368.
- [15] 于顺禄, 白仁骁, 郭若霖, 等. 骨重建过程“四环素活体标记”骨组织形态计量学指标在骨质疏松中的应用 [J]. 中国骨质与图像分析, 2003, 8(2):119–123.
- [16] Siler U, Rousselle P, Muller CA, et al. Laminin gamma chain as a stromal cell marker of the human bone marrow microenvironment [J]. *Br J Haematol*, 2002, 119(1):212–220.

(收稿日期:2014-01-28;编辑:段佳)